OXFORD

SOT | Society of Toxicology
www.toxsci.oxfordjournals.org

TOXICOLOGICAL SCIENCES, 2017, 1–13

doi: 10.1093/toxsci/kfx277
Advance Access Publication Date: December 15, 2017
Research Article

Brain Vacuolation Resulting From Administration of the Type II Ampakine CX717 Is An Artifact Related to Molecular Structure and Chemical Reaction With Tissue Fixative Agents

Richard Purcell,[*,1] Gary Lynch,[†] Christine Gall,[†] Steven Johnson,[‡] Zhong Sheng,[§] Michael Rajesh Stephen,[¶] James Cook,[¶] Robert H. Garman,[‖] Bernard Jortner,[‖‖] Brad Bolon,[‖‖‖] Daniel Radin,[*] and Arnold Lippa[*]

[*]SVP R&D, RespireRx Pharmaceuticals, Inc, Glen Rock, New Jersey 07452; [†]University of California Irvine, Irvine, California; [‡]SAJ Pharmaconsulting, LLC; [§]PsychoGenics Inc, Tarrytown, New York; [¶]University of Wisconsin- Milwaukee, Wisconsin; [‖]Consultants in Veterinary Pathology, Murrysville, Pennsylvania; [‖‖]Virginia Tech, Blacksburg, Virgina; and [‖‖‖]GEMpath Inc, Longmont, Colorado, 80504

[1]To whom correspondence should be addressed at SVP R&D, RespireRx Pharmaceuticals Inc., 126 Valley Road, Glen Rock, NJ 07452. Fax: (201) 493-0887. E-mail: rpurcell@respirerx.com.

ABSTRACT

Ampakines are small molecule positive allosteric modulators of the alpha-amino-3-hydroxy-5-methyl-4-isoxazolepropionic acid (AMPA). One class II ("low impact") ampakine, CX717, has been implicated to have a neurotoxic effect based on findings in nonclinical, long-term toxicity studies. The neurotoxicity concerns, which halted the clinical development of the molecule, arose due to a finding of extensive white matter vacuolation in multiple brain regions of animals that were administered high doses of CX717 in several test species (unpublished data). This work characterized the features and a potential mechanism by which ampakines induce vacuoles in brain tissue. Brain sections from adult rats given CX717 (750 mg/kg BID by oral gavage) exhibited no vacuoles with acute or short-term dosing. However, after 14 or more days of treatment, vacuoles were prominent in cerebellum, globus pallidus, and hippocampus. Vacuole margins were lined by glial fibrillary acidic protein (GFAP), and by transmission electron microscopy were shown to be astrocyte processes. CX717-associated vacuoles occurred in formaldehyde-fixed specimens but not flash-frozen samples. Time-course experiments showed that brain tissue slices from CX717-treated animals exhibit no vacuoles until immersed in formaldehyde fixative, whereupon vacuoles form and expand in a time-dependent manner. Chemical interactions in test tube experiments have demonstrated that the combination of CX717 and formalin in an aqueous solution produces an exothermic reaction. Taken together, the data indicate that CX717 does not induce vacuoles in vivo, but rather is associated with astrocyte vacuolation *post mortem*, likely as the ampakine reacts with formalin to produce gas pockets in brain parenchyma.

Key words: ampakine; artifact; brain; translational medicine; vacuolation.

The alpha-amino-3-hydroxy-5-methyl-4-isoxazolepropionic acid (AMPA) receptor mediates the majority of fast glutamatergic transmission in the central nervous system, and therefore represents an excellent target to enhance neuronal signaling. Ampakines are small molecule, positive allosteric modulators of the AMPA receptor that readily cross the blood-brain barrier to potentiate glutamate signaling. A number of ampakine molecules have been evaluated in human clinical trials as potential

therapies for a variety of neurological disorders including Alzheimer's disease (Danysz, 2002), attention deficit/hyperactivity disorder (Rueda *et al.*, 2009), depression (Kara *et al.*, 2015), schizophrenia (Goff *et al.*, 2008, opiate-induced respiratory depression (Oertel *et al.*, 2010; Ren *et al.*, 2009), sleep deprivation (Wesensten *et al.*, 2007), and sleep apnea (unpublished data). Although select ampakines have demonstrated therapeutic potential in clinical trials, to date, no ampakine molecule has been approved for clinical use.

The ampakines can be grouped into two classes based on the chemical scaffold upon which each class has been designed. The high-impact or class I ampakines are based on cyclothiazide, and bind to the cyclothiazide-binding site on the AMPA glutamate receptor. The high impact molecules prolong deactivation and inhibit desensitization, thus prolonging synaptically evoked neuronal response duration. The low-impact or class II ampakines are based on the structure of aniracetam, do not bind to the cyclothiazide-binding site, and primarily increase amplitude of synaptic responses of neurons. Kinetic receptor modeling demonstrates that high-impact ampkines primarily slow AMPA receptor channel closing, whereas low-impact ampakines preferentially accelerate channel opening (Arai and Kessler, 2007). The low-impact ampakines, including CX717, CX1739, and CX1942 potentiate field excitatory postsynaptic potentials (fEPSPs) in hippocampal slice neurons, increasing amplitude of response by roughly 25%–30%. This neuronal response is in direct contrast to the high-impact ampakines, which increase fEPSPs by 300% or more, and therefore provoke seizures at high concentrations. It is postulated that the classes I and II ampakines are differential biased agonists of the AMPA glutamate receptor, which acts not only as a gated ion channel to promote neuron firing, but also through G-Protein signaling mechanisms that facilitate long-term potentiation, neurochemical response, and other downstream cellular processes (Ingvar *et al.*, 1997, Lynch and Gall, 2013).

Results of preclinical and clinical studies demonstrate that the class II ampakines have comparable potencies of 5–15 mg/kg in both animal models and in humans for enhancing attention, improving cognition, and preventing opioid induced respiratory depression (Greer and Ren, 2009; Haw *et al.*, 2016; Ingvar, 1997; Oertel, 2010; Silverman *et al.*, 2013; and data on file).

One key challenge in the clinical development of ampakines has been the concern that these neuroactive agents may elicit neurotoxicity. The ampakines currently in clinical development include the class II or "Low Impact" (Arai *et al.*, 2002; Greer and Ren, 2009) molecule CX717. The safety concerns about ampakines arose during the clinical development of CX717 based on findings in long-term nonclinical toxicity studies (unpublished data). In 90-day rat and nonhuman primate dose escalation studies, microscopic evaluation of brain sections demonstrated that animals treated repeatedly with high doses of CX717 for several weeks or longer consistently exhibited prominent vacuoles in brain parenchyma when evaluated using standard histopathologic methods. Although not associated with in-life neurological dysfunction, the extent of vacuolation led to the delay of further development of CX717 until the pathogenesis of the vacuolation could be defined.

We note that vacuoles in brain parenchyma are a common histopathologic finding that can result from several potential mechanisms associated with excitotoxicity, prion diseases, and spongiform encephalopathies. For example, neuronal injury leading to cell death and disintegration is a means by which classical excitotoxic molecules (eg, domoic acid, kainic acid) may produce spaces in brain domains with vulnerable neuron populations, especially the cerebral cortex, cerebellum, and hippocampus (Strain and Tasker, 1991). Parenchymal vacuolation (or "spongiform degeneration" of axons and/or neuron cell bodies) is a chronic consequence of neuron infection with prion particles (Ye and Carp, 1996). These types of vacuoles caused by neurotoxins or infection are associated with neuronal degeneration, which is not found in CX717 treated animals. Alternatively, vacuoles may develop by accumulation of fluid within astrocyte processes (Garman, 2011) or myelin (Peters, 2009), and artefactual vacuoles may arise by extraction of white matter constituents during routine tissue processing, especially an extended holding period in alcohol during the paraffin infiltration step of embedding (Rastogi *et al.*, 2013).

Understanding that certain neurotoxic and infectious mechanisms of vacuolation represent genuine lesions to astroglia that are essential to neuroprotection and normal function (Bélanger and Magistretti, 2009, Kimmelberg and Nedergaard, 2010), and therefore would thwart development of a new neuroactive molecule, the current studies were undertaken to investigate the specific mechanisms by which ampakines elicit brain vacuoles and to explore the functional impact of vacuole induction. Our hypotheses, based on the absence of clinical signs of neurological dysfunction associated with neuronal damage, were that (1) the brain vacuolation induced by CX717 arises from an interaction of the test article with reagents involved in tissue fixation and/or processing rather than through any inherent neurotoxic potential of the ampakine class, and that (2) the affected neural cells are of glial origin. To test these hypotheses, we conducted a series of *in vitro*, *ex vivo*, and *in vivo* experiments. Based on our robust dataset, we now can show that CX717-induced brain vacuoles are artifacts arising in astrocytes *post mortem* through an exothermic reaction of the ampakine with formalin during tissue fixation.

MATERIALS AND METHODS

Ethical Treatment of Animals

The animal work was conducted as a series of studies between 2006 and 2007 and in 2015 in accordance with then extant federal (*Guide for the Care and Use of Laboratory Animals*, 2001) and relevant International Conference on Harmonization (ICH S6 R1, 1997) Harmonized Tripartite Guidelines using generally accepted methods for testing pharmaceutical compounds as set forth in "Principles for the Utilization and Care of Vertebrate Animals Used in Testing, Research, and Training" (Federal Register, 1985). Experimental protocols for each study were approved in advance by the Institutional Animal Care and Use Committee.

Animals and Husbandry

Young adult, male and female Sprague-Dawley rats (Charles River Laboratories) were quarantined for one week before initiation of each study. All rats were housed ($n = 1$/cage) in filter-capped polycarbonate cages, supplied with commercial pelleted chow and filter-purified tap water *ad libitum*, and were housed in a room with constant temperature (21°C ± 2°C) and humidity (45% ± 10%). Animals were exposed to 12 h of light daily.

Ampakines

"Low Impact, Class II" Ampakines designated CX717, CX1739, or CX1763 (active metabolite of CX1942, a prodrug ester) (Figure 1) were utilized as test articles. These agents have a common oxadiazole N-oxide structure, varying based on the arrangement of

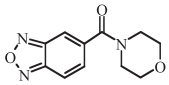

CX717
1-(benzofurazan-5-ylcarbonyl)morpholine

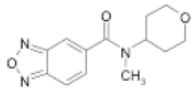

CX1739
N-Methyl-N-(tetrahydro-2H-pyran-4-yl)-2,1,3-benzoxadiazole-5-carboxamide

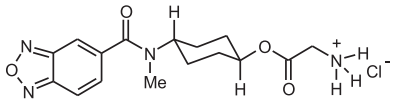

CX1942/CX1763
trans-4-[(2,1,3-Benzoxadiazol-5-ylcarbonyl)(methyl)amino] cyclohexyl glycinate Hydrochloride

Figure 1. Chemical structures of CX717, CX1739, and CX1763.

their rings and side groups. All ampakines were solubilized in 0.5% methylcellulose and 0.1% Tween 20 ("vehicle") for *in vivo* and *ex vivo* studies.

In Vivo Studies

Ampakine treatment in rats. Ampakines were administered *in vivo* at total daily doses of 1500 (CX717), 750 (CX1739), or 1000 (CX1763) mg/kg body weight/d. Agents were given in 2 equal doses by oral gavage at an interval of 8 h. An acute dose study of CX1739 was conducted at doses up to 1500 mg/kg. In-life procedures and necropsies were performed at MPI Research (Mattawan, Micigan).

Ampakine treatment in monkeys. CX717 was administered to in BID doses of 0, 75, 125, 225, and 300 mg/kg to Cynomolgus monkeys daily for 90 consecutive days. Agents were given in two equal doses by oral gavage at an interval of 8 h. In-life procedures and necropsies were performed at MPI Research (Mattawan, Micigan).

Brain processing. Immersion Protocol. At necropsy, animals were deeply anesthetized with sodium pentobarbital (by intraperitoneal [IP] injection) and then decapitated. The mandible was detached, the skin and calvaria were removed to expose the brain, and the head was fixed by immersion in either neutral buffered 10% formalin (NBF) containing methanol as a stabilizing agent or in modified Karnovsky's fixative (4% methanol-free formaldehyde [MFF, freshly reconstituted from paraformaldehyde powder] plus 0.2% glutaraldehyde in a 0.1 M phosphate buffer, pH 7.4). Brains were fixed *in situ* for at least 72 h prior to transfer (by overnight shipping in fixative) to the histology facility.

Perfusion Protocol. At necropsy, animals were deeply anesthetized with sodium pentobarbital IP, and a thoracotomy was performed to expose the heart. Solutions were introduced through a 16-gauge needle placed in the left ventricle, while fluids were drained from an incision in the right atrium. Fixation was undertaken by introducing ice-cold phosphate-buffered saline (0.1 M, pH 7.4) for two minutes followed by one of three fixatives: 4% MFF in 0.1 M phosphate buffer, pH 7.4; modified Karnovsky's solution (4% MFF/0.2% glutaraldehyde in 0.1 M phosphate buffer, pH 7.4); or glacial acetic acid/ethanol (1: 6). Fixatives were perfused at room temperature (RT) for 10–15 min, with one exception noted below. Solutions were perfused at constant pressure using gravity. Following perfusion, heads were removed, the calvaria was removed, and the whole head was immersed in the same fixative. Brains were fixed overnight *in situ* at 4 °C; brains fixed in glacial acetic acid/ethanol were transferred to NBF after 2 h prior to overnight refrigeration. Two special steps were employed for certain MFF-fixed brains. First, some animals were perfused with AQIX (AQIX, London, UK), a solution designed to extend tissue viability time when shipping donor organs, followed by ice-cold 4% MFF. Second, some MFF-fixed brains were cryoprotected in 30% sucrose (in 4% MFF) for shipping.

Freezing Protocol. At necropsy, animals were deeply anesthetized with sodium pentobarbital IP. The brain was removed rapidly (<45 s), flash-frozen in an isopentane bath cooled by floating dry ice chips, and then stored at –80 °C.

Brain Processing for Light Microscopic Analysis. All brains were shipped in fresh fixative or (for specimens destined for cryosectioning) on dry ice to the histology facility of Experimental Pathology Laboratories, Inc. (Research Triangle Park, North Carolina) or to Consultants in Veterinary Pathology, Inc. (Murrysville, Pennsylvania). Specimens were trimmed according to a recognized scheme (Garman *et al.*, 2001) to produce 8–11 coronal slices and embedded routinely in paraffin. Serial sections were stained with hematoxylin and eosin (H&E, to assess general tissue architecture); Fluoro-Jade B (FJB, to detect dying and dead neurons); or Bielschowsky's silver (to highlight neuron and axon degeneration). Brains sections from selected studies were also labeled by indirect immunohistochemistry to demonstrate the astrocyte marker glial fibrillary acidic protein (GFAP). Key structures available for analysis in brain sections from all animals were cerebral cortex (frontal, parietal, piriform, temporal, occipital); striatum (including caudate, globus pallidus, and putamen); hippocampus; thalamus; hypothalamus; midbrain (colliculi and periaqueductal gray); cerebellum; pons; and medulla oblongata.

Brain Processing for Ultrastructural Analysis. Selected blocks of globus pallidus and cerebellum (ie, the two most affected brain regions following extended high-dose CX717 treatment) from some perfusion-fixed brains were shipped overnight in modified Karnovsky's fixative to the Laboratory for Neurotoxicity Studies at the Virginia-Maryland Regional College of Veterinary Medicine (Blacksburg, Virginia). Blocks were post-fixed by immersion in 3.0% glutaraldehyde in 0.1 M phosphate buffer, pH 7.4 for 2 h at 4 °C; postfixed again by immersion in 0.1% osmium tetroxide for 1 h at 4 °C; and then processed into PolyBed epoxy resin according to the manufacturer's instructions. Multiple blocks per rat ($n = 2$ control and 2 CX717-treated) were sectioned at 1 micron and then stained with toluidine blue and safranin. Following a noncoded (nonblinded) evaluation by light microscopy, thin sections (approximately 50-nm thick) from one representative block per rat were stained using lead citrate and uranyl acetate and then examined using a Zeiss 10CA transmission electron microscope. Cytoarchitectural changes were evaluated against the expected ultrastructural appearance (Peters *et al.*, 2008) of neurons and glia. Ultrastructural images included in this article were edited slightly but globally using Adobe Photoshop CS2 to enhance brightness and contrast.

Brain Processing to Evaluate the Relationship Between Anesthesia and Tissue Handling Techniques. Brains were handled in four different ways as follows: (1) rats were anesthetized with sodium pentobarbital, decapitated, and their brains fixed

by immersion in 10% NBF; (2) rats were decapitated without prior anesthesia and the brains similarly fixed by immersion in NBF; (3) rats were anesthetized with sodium pentobarbital after which the brains were rapidly removed and "snap frozen" in a mixture of dry ice and isopentane; (4) rats were decapitated without prior anesthesia and the brains similarly "snap frozen" in a mixture of dry ice and isopentane. Two coronal slices were prepared from each of the frozen brains—one at approximately the level of the anterior commissure and the other through the middle of the cerebellum. All tissues were processed for either cryosectioning (frozen coronal slices) or for paraffin (immersion-fixed brains). Nine coronal slices were prepared from each of the immersion-fixed brains and these slices multiply-embedded within two paraffin blocks. Eight cryostatic step sections were prepared from each of the frozen brains—5 from the region of the striatum and three through the cerebellum. All sections were stained with hematoxylin and eosin (H&E) for microscopic evaluation. Photomicrographs were collected in Nikon Electronic Format (NEF) and were then batch-converted to JPEG format using Nikon Capture software. Photomicrographs were resized in Adobe Photo Shop CS and arrows added where appropriate. Other than for the addition of arrows and for slight sharpening or contrast enhancement, no digital manipulations were performed on the images. In addition to the photomicrographs, selected histologic sections were scanned using a Nikon Super Coolscan 4000 slide scanner along with a microscope slide adapter. These scans were similarly adjusted slightly for contrast and sharpened in Adobe Photo Shop CS.

Ex Vivo *Studies—Tissue Slice Preparations*

Ampakine treatment. Rats were treated with CX717 *in vivo* at 1, 500 mg/kg body weight/d for 14 days in the animal facility of Cortex Pharmaceuticals (Irvine, California), after which live animals were transported to the Gillespie Neuroscience Research Facility at the University of California—Irvine (Irvine, California). Agents were given in two equal doses by oral gavage at an interval of 8 h.

Brain removal and sectioning. Rats were deeply anesthetized with sodium pentobarbital IP and then decapitated. Whole brains were removed rapidly (45 s) and immediately sliced.

Slice Preparation. Slices (140 or 350 μm thickness) were prepared on a Leica Vibroslicer and maintained on three separate electrophysiological recording set-ups using conventional slice recording techniques (Kramer *et al.*, 2004). All sections assessed were alive and healthy after cutting as indicated by electrophysiological evaluation. Slices were kept in oxygenated artificial cerebral spinal fluid (aCSF) until use. The composition of the aCSF (in mM) was 124 NaCl, 3 KCl, 1.25 KH_2PO_4, 2.5 $MgSO_4$, 3.4 $CaCl_2$, 26 $NaHCO_3$, and 10 glucose (Kramar *et al.*, 2004). The aCSF was maintained at 31°C (±1°C).

Slice Allocation. Slices allocated to electrophysiological analysis (see below) were distributed to 2 whole-cell recording chambers, where they were submerged and perfused with constantly recirculating, oxygenated aCSF, and to an interface chamber designed for extracellular recording; in the latter slices were maintained in an interface configuration with constant aCSF bath perfusion and the upper face of the slice exposed to a O_2/CO_2 atmosphere. The aCSF in all chambers was maintained at 31°C (±1°C). Following or in lieu of electrophysiological recording, tissue slices were processed using one of 3 histological procedures (see below) to permit microscopic examination.

Electrophysiological analysis. Microscopy. Infrared photomicroscopy was used in association with whole-cell recordings. For the extracellular recording cases, the slices were removed from the chamber, placed on a slide in warm aerated aCSF, and photographed with a high-resolution, wide angle, bright field microscope. Low- and high-magnification photomicrographs were collected from multiple sites within the globus pallidus and striatum (ie, caudate/putamen) in all specimens. This array of procedures was used in an effort to sample as much tissue as possible from a given animal.

Recordings. Whole cell recordings were made from visually identified neuronal cell bodies. Cells in the target region were substantially smaller than the vacuoles observed during previous histopathologic evaluations (unpublished data); accordingly, vacuoles, if present, were detectable by the experimenters. Two types of electrophysiological data were collected: (1) evoked responses (ie, excitatory postsynaptic currents [EPSCs] and inhibitory postsynaptic currents [IPSCs]) for the whole cell clamp recordings, and excitatory field potentials [EPSPs] for extracellular recordings) elicited by stimulation of the fascicles of axons running through the striatum; and (2) spontaneous EPSCs and IPSCs in the whole cell clamp recordings. Recordings were collected for responses evoked in the (a) cortical-striatal system with recordings made in the caudate/putamen (traces designated "striatum" or "CPu") and (b) the striato-pallidal system with recordings collected from the globus pallidus (traces designated "globus pallidus" or "GP"). Traces were collected for each projection system from 4 ampakine-treated and 2 vehicle-treated rats.

Preparations demonstrated that evoked responses can be recorded using both whole cell and field recording techniques in all animals. Functional status of AMPA-mediated signaling in brain slices was confirmed by spiking the aCSF with 10 mM of DNQX (6, 7-dinitroquinoxaline-2, 3-dione; (Sigma-Aldridge, St. Louis, MO), an AMPA and kainate receptor antagonist.

Neurohistological analysis. In most rats, adjacent slices were prepared using two or all three methods to demonstrate concordance of the findings across neurohistologic procedures.

Technique No. 1 was to produce unfixed sections by removing a freshly acquired 350-μm-thick slice from the vibratome, rapidly freezing it on a −25°C platform, and then producing 20- to 25-μm thick cryostat sections. These sections were air-dried at 20°C and only then immersion-fixed for 15 min at 20°C in 4% MFF in 0.1 M sodium phosphate buffer, pH 7.4 prior to H&E staining.

For Technique No. 2, freshly acquired or reallocated (ie, previously used for electrophysiological recording), 350-μm thick slices were fixed overnight, cryoprotected by immersion in 20% sucrose in 0.1 M sodium phosphate buffer for 20–60 min at 4°C, and then sectioned at 25 μm. These sections were air-dried at 20°C and only then immersion-fixed for 15 min at 20°C in 4% MFF in 0.1 M sodium phosphate buffer, pH 7.4 prior to H&E staining.

Technique No. 3 evaluated the time-course for vacuole formation by placing freshly acquired, 140-μm thick slices on microscope slides and then examining them after either air-drying at 20°C only (ie, unfixed) or after air-drying at 20°C followed by immersion fixation for 1–30 min prior to rinsing in 0.1 M sodium phosphate buffer, pH 7.4. Sections were stained with cresyl violet, which emphasizes neuronal populations.

In Vitro *Studies—Mechanistic Chemistry*

Chemistry experiments were conducted in 3-neck (25 ml) round bottom flasks using 1.5, 15, and 16.5 ml, respectively, of the final

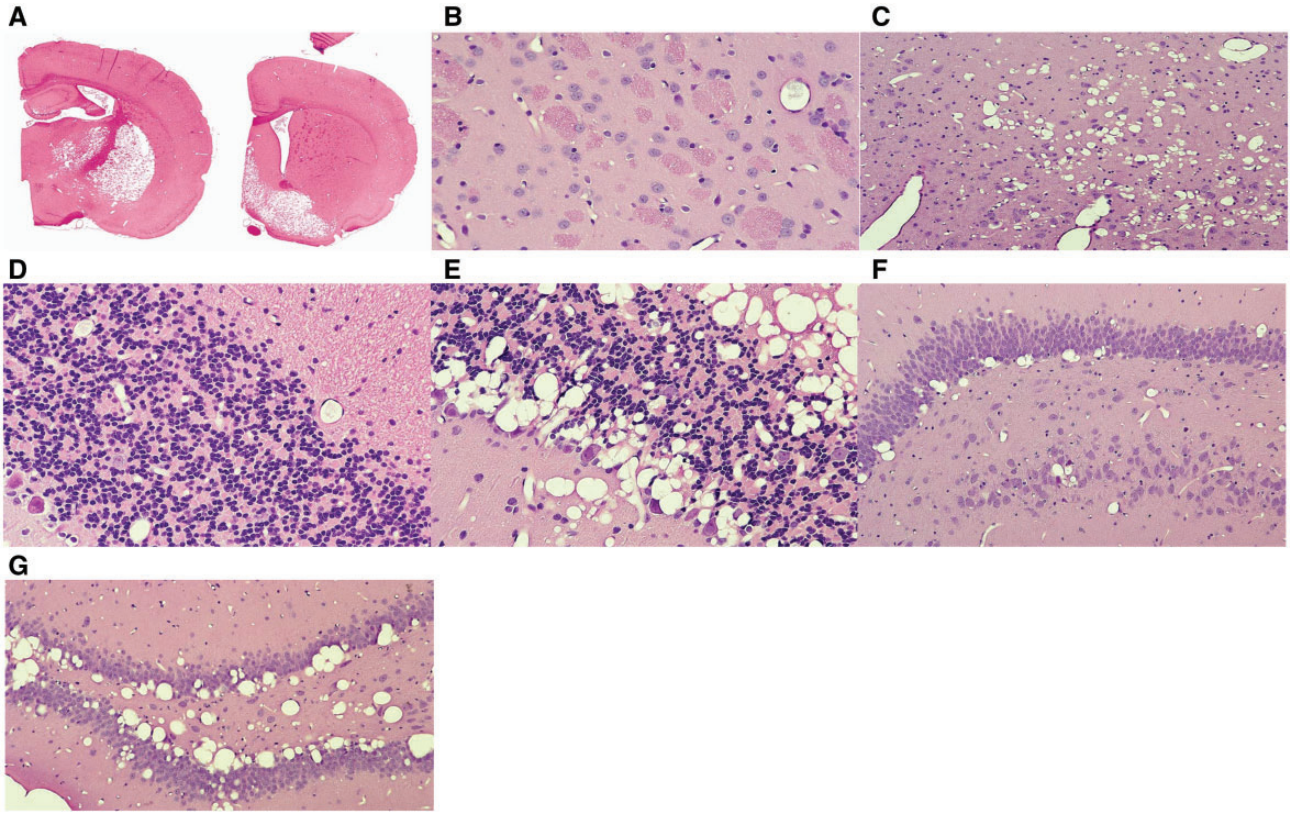

Figure 2. Distribution of CX717-induced Brain Vacuoles. A, Vacuolation is extensive as indicated by clear spaces in the basal ganglia at the level of the globus pallidus and rostral (anterior) thalamus (section on left) and the caudate-putamen (section on right). Vacuolation also involves the dentate gyrus of the hippocampus to a lesser degree (section on left). B, Globus pallidus from a control male demonstrating normal structure. C, Globus pallidus of a CX717-treated male rat with vacuolation. D, Cerebellar cortex from a control male rat showing normal structure. E, Cerebellar cortex of a CX717-treated male rat showing abundant vacuolation as a band of clear vacuoles in the Purkinje neuron layer (lower left), diffusely in the white matter (upper right), and scattered within the granule cell layer (middle). Despite prominent vacuolation, all of the Purkinje and granule neurons are cytologically normal in appearance. F, Dentate gyrus of the hippocampus of a CX717-treated male rat showing scattered vacuoles along the base of the upper blade of the granule neuron layer. G. Dentate gyrus of the hippocampus from a separate CX717-treated animal to demonstrate the substantial inter-animal variation in treatment-related vacuolation. Samples: brain from rats givens vehicle or CX717 for 3 months. Processing: Formalin fixation by perfusion, paraffin embedding, H&E stain.

reaction mixtures for each test article (defined blow). Solutions began at RT (ie, initial temperature of reaction mixture, as measured at 0 min for each independent experiment). With solutions undergoing constant stirring, the temperature was measured continuously for 30 min with a K-type thermocouple using a Fluke multimeter (Fluke Biomedical Division of Fluke Electronics Corporation, Everett, Waltham).

In the first series, the reaction mixture consisted of CX717 (2.04 g) added to 1.5 ml of methanol. In a second series, the reaction mixture was CX7I7 (2.04 g) added to 15 ml of NBF (freshly prepared according to Aldrich product specifications). In the third series, the reaction mixture combined CX717 (2.04 g) with 1.5 ml of methanol, followed immediately by the addition of 15 ml of NBF.

RESULTS

Character of CX717-Associated Brain Vacuolation

Long-term, high-dose treatment with CX717 results in the appearance of vacuoles in multiple brain regions (Figure 2). The globus pallidus was affected most extensively, but prominent

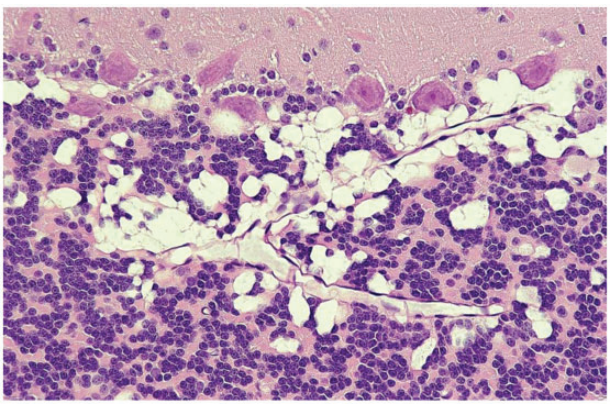

Figure 3. Vacuoles track along neurons and blood vessels. Cerebellum from a female monkey showing moderate vacuolation within the Purkinje neuron layer and underlying granule cell layer. Note how the vacuoles track along a Y-shaped blood vessel that extends through both of these affected neuron layers, and that the neurons adjacent to vacuoles exhibit no evidence of degeneration or necrosis. Samples: brain from a cynomolgus monkey given oral doses of CX717 (300 mg/kg BID) for 3 months. Processing: Formalin fixation by perfusion, paraffin embedding, H&E stain.

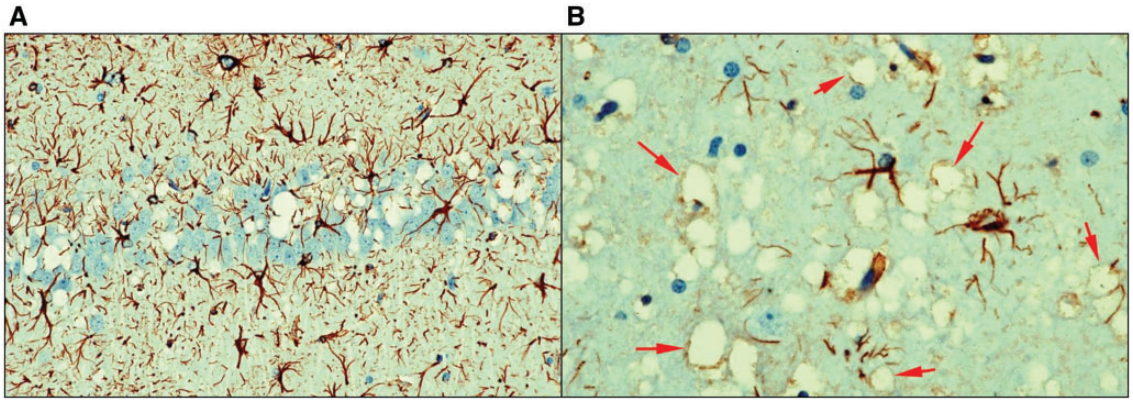

Figure 4. Vacuoles occur in astrocytes in the absence of astrocyte hypertrophy/hyperplasia. A, CA1 pyramidal neuron layer of the hippocampus of a CX717-treated rat demonstrating moderate vacuolation in the absence of astrocyte hypertrophy and hyperplasia as well as neuron degeneration. B, Ventral globus pallidus from a CX717-treated rat showing that numerous vacuoles are bordered by thin rims labeled by GFAP (arrows) in the absence of astrocyte hypertrophy or hyperplasia. Samples: brains from rats given CX717 for 3 months. Processing: Formalin fixation by perfusion, paraffin embedding, indirect immunohistochemistry to detect GFAP (an astrocyte marker), hematoxylin counterstain.

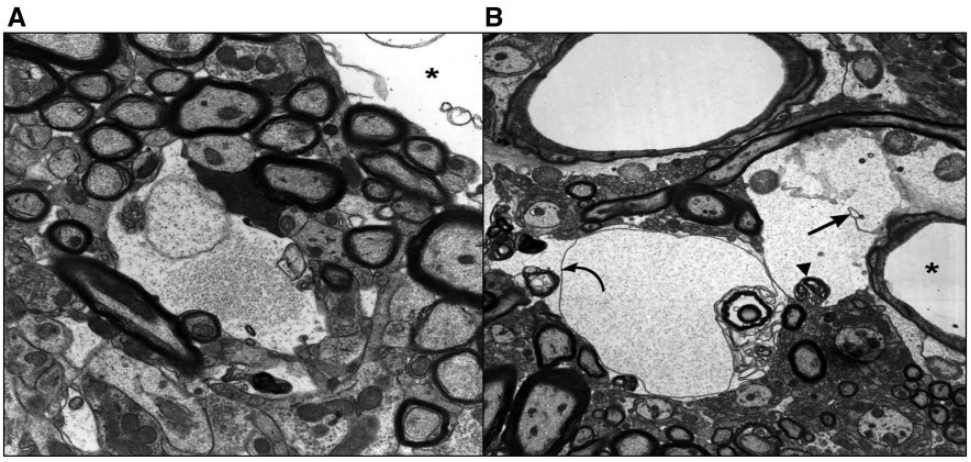

Figure 5. Vacuoles represent swollen astrocytes. A, Early stage of vacuole formation is indicated by pale-staining cytoplasmic swelling of an astrocytic process encircled by a bundle of myelinated nerve fibers (magnification 5000×). There is separation of a bundle of filaments and membranes and vesicular bodies in the cell. Part of a larger vacuole is present at the upper right (*). Adjacent myelinated fibers are intact. B, Later evolution of vacuoles is showcased by a large, pale-staining perivascular vacuole adjacent to a capillary (*). This vacuole has a multiloculated profile with focal rupture of a thin intercellular septum (arrow). There is protrusion of a membranous body from an adjacent neurite (arrowhead). A membrane encloses a portion of the vacuole (curved arrow). Samples: transmission electron micrographs of brain from a rat given 1500 mg/kg CX717 for 14 days. Processing: Formalin fixation by perfusion, post-fixation by glutaraldehyde and osmium tetroxide, embedding in epoxy resin, lead citrate, and uranyl acetate staining.

vacuolation also occurred (in descending order of severity) in the ventral pallidum and basal forebrain, cerebellar cortex (chiefly the Purkinje neuron layer), deep cerebellar nuclei, hippocampus, thalamus, midbrain, and caudate-putamen (ie, striatum). Other brain regions affected in some animals (especially males) included cerebral cortex, the septal nuclei, nucleus accumbens, stratum compactum of the substantia nigra, and the amygdala. Vacuole severity was greater in animals treated at higher doses and/or for longer periods of time. Lesions typically were bilaterally symmetrical. Vacuole severity was variable but typically was moderate or marked.

Vacuoles appeared within neuropil and myelinated fiber bundles as single or grouped, oval to round, colorless spaces. At the light microscopic level, vacuoles were not present within the neuronal cytoplasm but instead occurred adjacent to neurons—sometimes compressing their soma—and tracking along small blood vessels (Figure 3); this distribution suggested that the vacuoles might represent swollen astrocytic processes. Vacuoles were not associated with hypertrophy or hyperplasia of GFAP-expressing astrocytes, but thin GFAP tendrils bordered many but not vacuoles (Figure 4), thereby reinforcing the likelihood that vacuoles represent swollen astrocytic processes.

At the ultrastructural level, vacuoles in the globus pallidus exhibited a sequence of changes by which nascent vacuoles expanded into large spaces. In early stages, affected astrocytes were swollen, as shown by separation of organelles and filament bundles, and had electron-lucent ("pale") cytoplasm (Figure 5). These swollen perivascular cells developed large, membrane-limited intracellular spaces, some of which contained residual bundles of filaments or fine granular material but few organelles. In later stages, vacuoles developed multiloculated profiles subdivided by thin membranous septae. Over time, outer membranes and internal septae within affected astrocytes often ruptured, which on occasion allowed

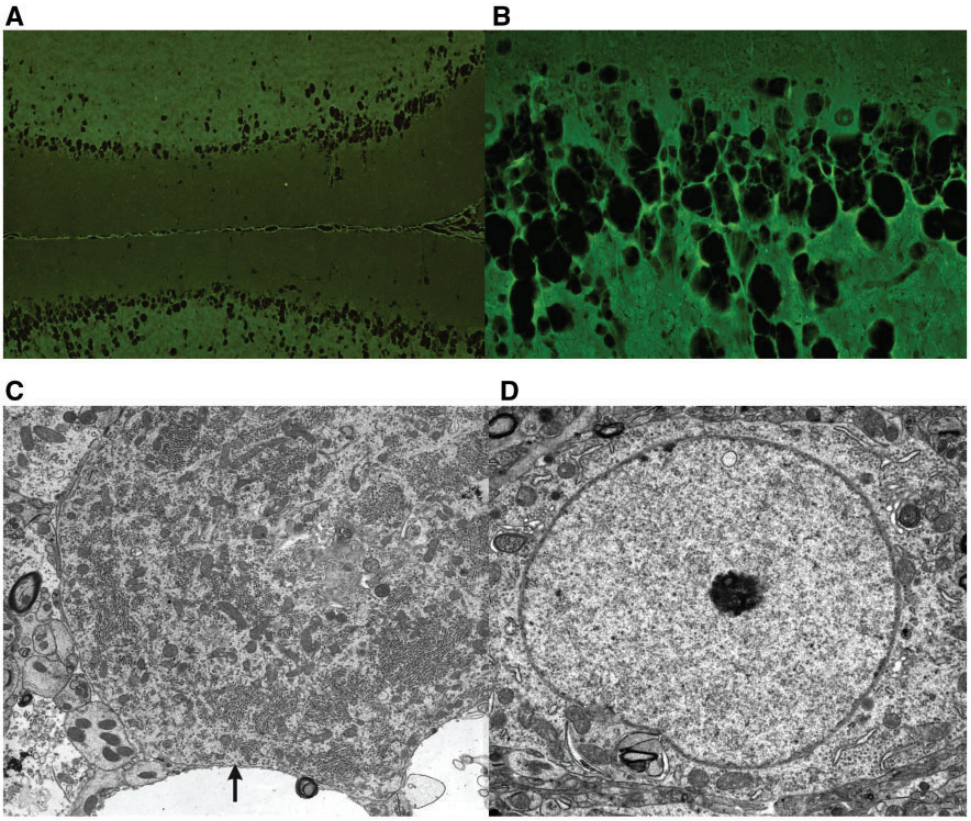

Figure 6. Neurons in vacuolated regions are not affected. A and B, Cerebellar cortex of a CX717-treated male monkey stained with FJB, a stain utilized to demonstrate neuronal degeneration and necrosis. Although large numbers of vacuoles (black spaces) are present in the Purkinje neuron and granule neuron layers (pale green parenchyma), there is no evidence of neuronal degeneration or death (ie, bright green Fluoro-Jade staining). C, Intact Purkinje cell body (arrow) adjacent to vacuoles (magnification 5000×). D, Intact granule cell neuron in an affected region (magnification 6300×). Samples: brains from monkeys given CX717 (300 mg/kg BID) for 3 months. Processing, Fluoro Jade B: Formalin fixation by perfusion, paraffin embedding, Fluro Jade B. Processing, electron microscopy: Formalin fixation by perfusion, postfixation by glutaraldehyde and osmium tetroxide, embedding in epoxy resin, lead citrate and uranyl acetate staining.

incorporation of small unmyelinated axon profiles into the vacuole.

A striking feature of CX717-associated vacuolation was the absence of neuronal injury. No evidence of neuron degeneration (Figs. 3 and 4) or death (Figure 6) was observed, even in neuroanatomic regions characterized by large numbers of vacuoles. Vacuoles often extended to and sometimes substantially compressed neuronal cell bodies, but the intrusion did not produce any cytoarchitectural changes within encroached neurons. Similarly, neither demyelination nor myelinated fiber degeneration was observed in neuropil.

Time Course and Permanence of CX717-Associated Brain Vacuolation

Vacuoles did not appear in any brain samples from any animals following CX717 administration for 1 or 7 days. In contrast, after 14 days, tissue samples from all CX717-treated rats exhibited para-neuronal and perivascular vacuoles in multiple brain regions. In animals treated for longer periods, the vacuoles appeared to increase in size, seemingly via fusion of previously smaller spaces, to yield lesions of moderate to marked grade. This confluence was not associated with edema of the adjacent neuropil, suggesting that the blood-brain barrier remained intact.

Vacuole severity was substantially reduced in tissue samples from animals allowed a recovery period. Fewer samples had vacuoles after two weeks without CX717 treatment, and brain samples from only one animal had any definitive vacuoles after eight weeks. The severity of vacuoles also receded over time, usually appearing as a minimal or mild change.

Impact of Fixation on CX717-Associated Brain Vacuolation

During *in vivo* studies, CX717-associated vacuoles in paraffin-embedded sections were detected only in brains that had been fixed in aldehydes. Vacuoles were more prominent in specimens fixed by immersion rather than by perfusion. Vacuoles also were larger where the initial fixative was an aldehyde rather than another fixative (eg, glacial acetic acid/ethanol). Vacuoles did develop in frozen sections if the tissues subsequently were fixed in aldehyde (Figure 7). In contrast, vacuoles did not occur in unfixed sections from CX717-treated rats or in vehicle-treated animals, regardless of the fixation regimen (Figure 7).

Ex vivo brain slice preparations from CX717-treated rats did not exhibit vacuoles in the absence of aldehyde fixation (Figure 8), during electrophysiological recording by both infrared and bright-field microscopy (140- or 350-μm thick sections) (Figure 9). If slices were fixed in aldehyde before sectioning, vacuoles did develop starting at 1–2 min after commencement of fixation (Figure 10). Vacuole numbers and sizes increased with the length of fixation (Figure 10).

Impact of CX717 Treatment on Electrophysiological Activity

Extracellular field recordings were performed on 4 CX717-treated and two vehicle-control animals. Representative

recordings from each animal evaluated are presented in (Figure 11). Recordings of input-output (I/O) curves of local field potentials collected in the caudate/putamen confirmed that slices from all animals exhibited robust synaptic responses. Antagonist application (DNQX) verified that the glutamatergic cortico-striatal projections were fully functional. Responses to stimulation of striatal projections emanating from the caudate/putamen were recorded within the globus pallidus (ie, the most susceptible brain region following CX717 treatment). Response amplitudes were stimulation-polarity independent (Figure 11A) and exhibited a positive relationship to stimulation intensity that reached a maximum as would be expected for synaptic responses (Figs. 11C–F). Responses recorded from slices from CX717-treated rats showed no discernable difference in the size or shape to responses relative to recordings collected from vehicle-treated animals (compare Figs. 11C–F).

Whole-cell electrophysiological recordings were performed within the caudate/putamen in slices from the same animals described earlier. Stable IPSCs were recorded in slices from all animals, and I/O curves measured from ampakine-treated animals were not different from vehicle-treated controls (Figs. 11G and 11H).

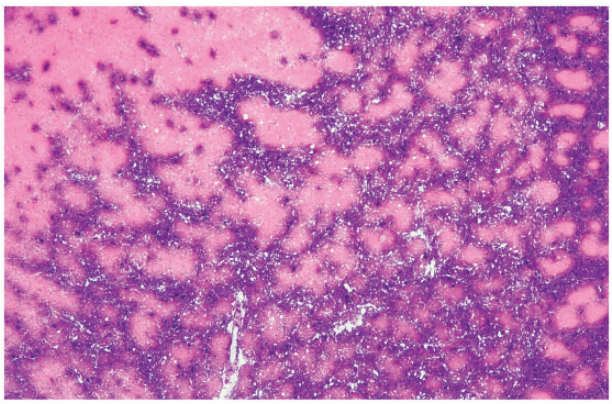

Figure 7. Vacuoles do not develop in tissue not exposed to aldehyde. Globus pallidus from a CX717-treated rat, demonstrating the absence of large vacuoles in cryosectioned tissue that was not fixed using an aldehyde-based solution. Samples: brains from rats given CX717 for 3 months. Processing: Rapid removal of unfixed brain, cryosectioning without prior fixation, brief fixation in isopentane, H&E stain.

Vacuologenic Potential of Other Ampakines

The possibility that class II ("low impact") ampakines as a drug class induce vacuoles in brain parenchyma was investigated by treating rats with other related molecules. Animals given either CX1739 (750 mg/kg/d BID) for 14 days or 4 weeks or CX1763 (1000 mg/kg/d BID) for 14 days did not develop neuropil vacuolation even though they had been processed routinely (Bolon *et al.*, 2013) by immersion fixation in NBF (Figure 12). As with CX717, these other class II ampakines did not elicit neuron degeneration or gliosis.

Interaction Between CX717 and Tissue-Fixing Agents: Potential Mechanism of Vacuole Induction

When CX717 was added to either a methanol- or formaldehyde-containing solution, no change in temperature was observed. However, when CX717 was added to a solution containing both methanol and formaldehyde (ie, a composition mirroring that of commercial NBF), a 7.3°C rise in temperature was recorded over a period of 30 min.

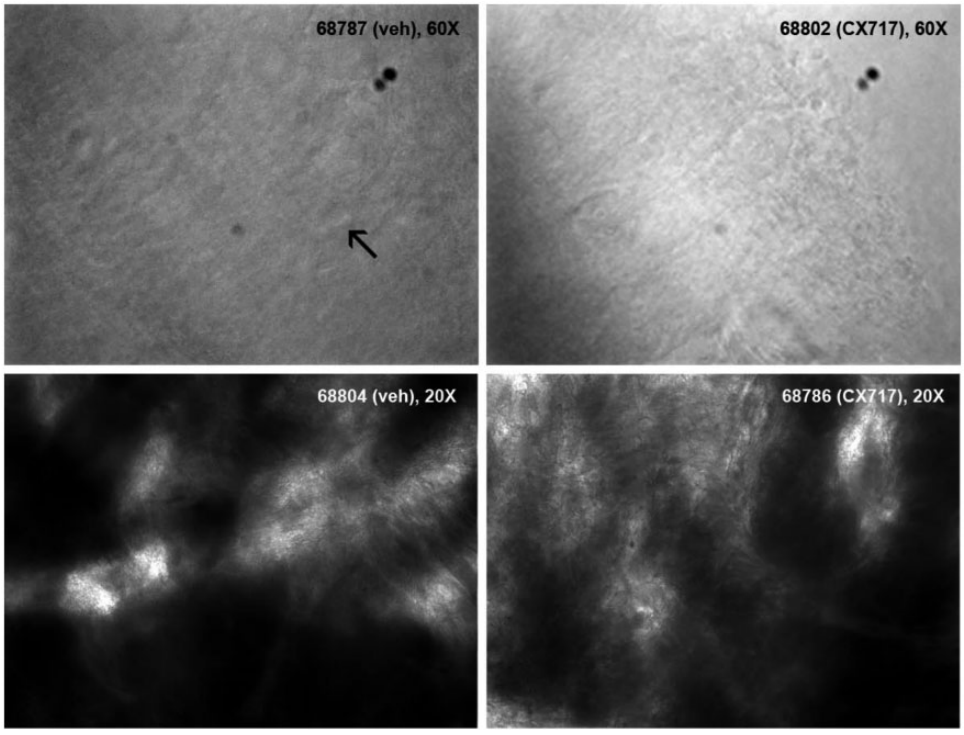

Figure 8. Vacuoles do not develop in unfixed living brain slices. Infrared (top) and bright-field (bottom) photomicrographs of the globus pallidus demonstrating a lack of vacuoles in living tissue from CX717-treated rats. Labels in the upper right corner of each image give the animal number, the treatment (CX717 or vehicle [veh]), and the objective magnification used to capture the image. The arrow in the vehicle-control panel (upper left) points to a neuronal cell body; physiologists clamp cells of this type. Vacuoles are several-fold greater in size than the indicated neuron, and thus would be apparent at this magnification if they had been present.

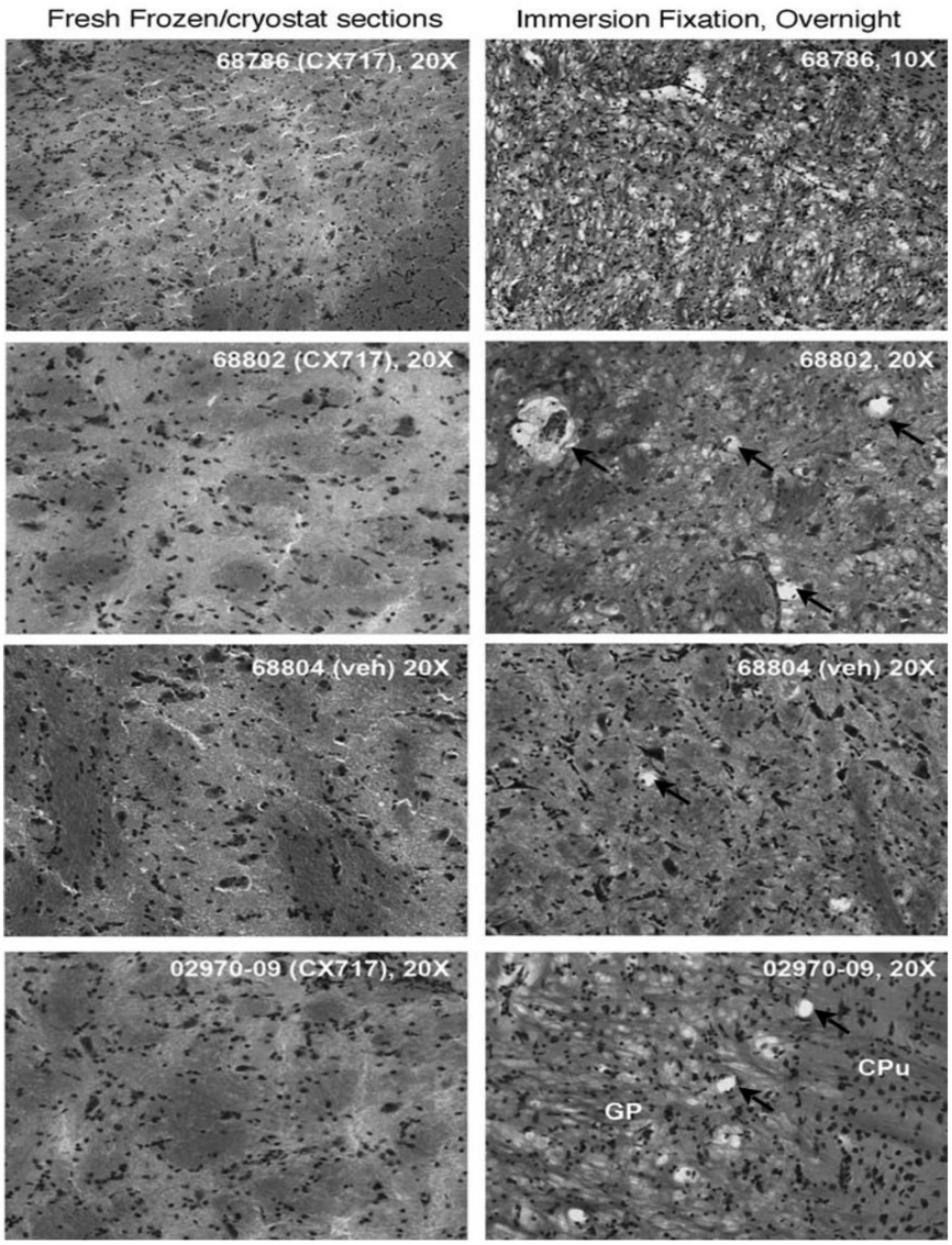

Figure 9. Vacuoles develop *post mortem* only in the presence of fixative. Photographs show (in each row) tissue slices through the globus pallidus of the same rat (eg, No. 68786 in the top row) that was quickly flash frozen without fixation (left column) or fixed by immersion in MFF (right column). As shown, vacuoles (arrows) appear when the living tissue is immersed in MMF (right) but are not apparent when the slice is quickly frozen without fixation (left). Labels in the upper right corner of each photomicrograph give the animal number, followed by the treatment (CX717 or vehicle [veh]), followed by the objective magnification used to capture the image.

DISCUSSION

As positive allosteric modulators of AMPA receptor-mediated glutamatergic neurotransmission, ampakines represent a promising new strategy for treating numerous human neurological diseases, including neurodegenerative, mood, psychiatric, and related disorders. However, efforts to develop the class II ("low impact") ampakine CX717 face current safety concerns and a previous regulatory hold due to the finding of widespread neuropil vacuolation in brain tissue samples from rats and monkeys following chronic treatment with high doses of the molecule. The current program of *in vivo*, *ex vivo*, and *in vitro* studies was undertaken to investigate whether or not this vacuologenic potential represents a class effect of such low-impact ampakines, and to define the pathogenic mechanisms responsible for generation of this finding. Our extensive data from numerous animal studies indicate that induction of neuropil vacuoles is a specific property of CX717 rather than a chemical class effect, and furthermore that these vacuoles represent a *postmortem* artifact of tissue processing rather than evidence of direct CX717-induced neurotoxicity. This interpretation is supported by multiple lines of evidence.

The anatomic characteristics of the CX717-associated vacuoles observed in tissues derived from *in vivo* treatment indicate that they arise in astrocytes rather than within neurons,

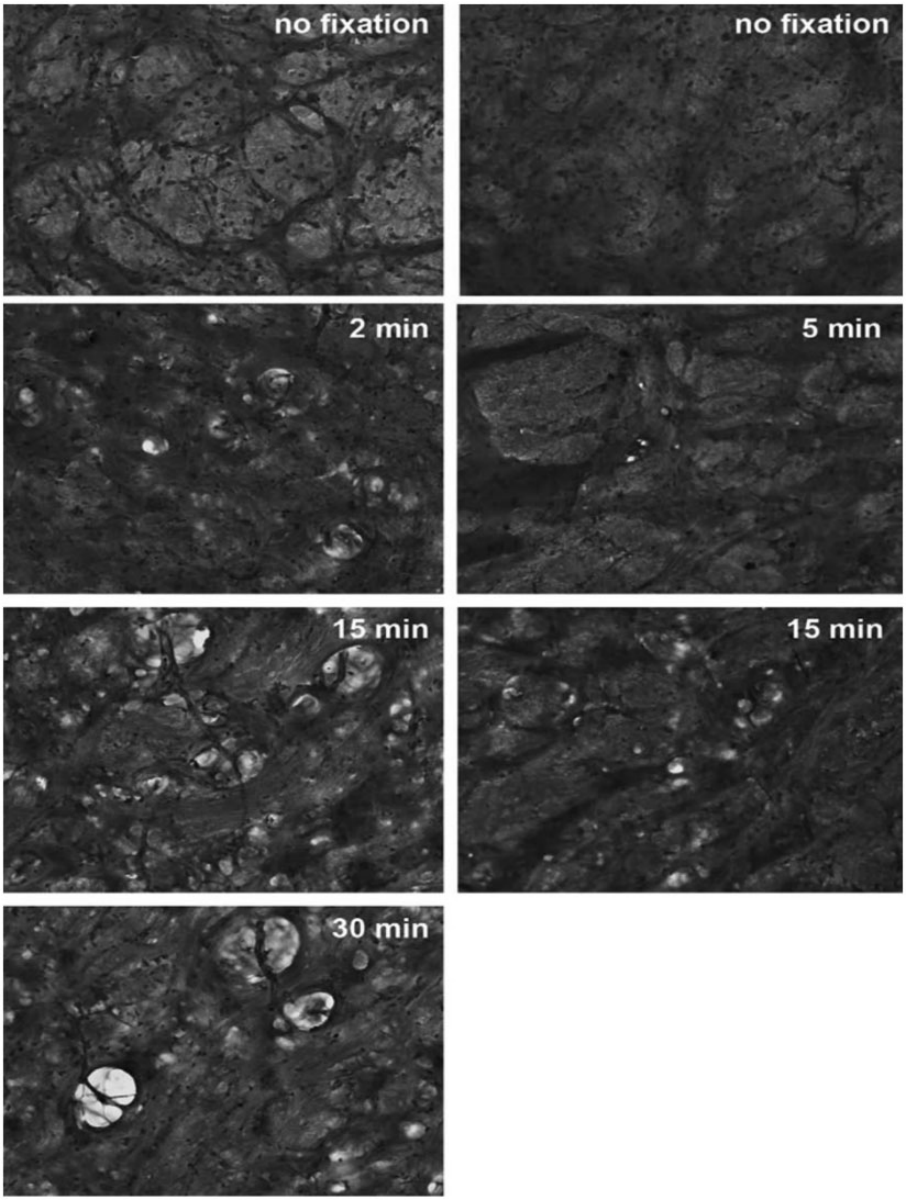

Figure 10. Vacuoles develop soon after fixation begins and increase in size over time. Vacuoles (bright spaces of variable size) appear after fixation is initiated in 140-μm-thick sections of globus pallidus from two CX717-treated rats (No. 69277, left column; No. 69262, right column) that were mounted on a microscope slide without fixation (top row) or after different fixation intervals. In both cases, vacuoles were absent in unfixed tissue (top row) in but increased progressively in numbers and size with time over 30 min. Some inter-animal variability in the severity of postfixation vacuolization is evident in these panels.

and are present in the perivascular space adjacent to blood vessels. At the light microscopic level, the vacuoles develop chiefly in neuropil and myelinated fiber bundles, often following the course of small capillaries. Many vacuoles are partially bounded by GFAP. By Transmission electron Microspcopy (TEM), the vacuoles may be identified as swollen, perivascular, glial cell processes. This distribution and molecular signature suggest that the affected cells are astrocytes and that vacuoles represent swollen astrocytic processes. Vacuoles may impinge on neuronal and glial nuclei, but they are not associated with visible degenerative changes or death of either of these neural cell types. Further, there are no effects on neuronal function as confirmed by electrophysiology. Although astrocytes express AMPA receptors (Fan *et al.*, 1999) that may be modulated by ampakines, glial reactions consistent with chronic chemically induced neurotoxicity (eg, astrocyte hypertrophy and hyperplasia with increased expression of GFAP) are absent in the brains of CX717-treated animals. This microscopic pattern suggests that the vacuoles do not represent a typical neurotoxic event (ie, leading to cell degeneration and death) but rather embody an unusual biologic manifestation leading to an enhanced vacuolation artifact.

Additional *in vivo* and *ex vivo* studies with brains of ampakine-treated rats reveals that vacuoles are artifacts associated with tissue processing conditions, specifically brain preservation in aldehyde-based fixatives. CX717-associated vacuoles developed following both immersion or perfusion procedures and were larger and more numerous as the length of fixation was increased. Vacuoles also were more pronounced if CX717 treatment was longer, and in the absence of a long post-

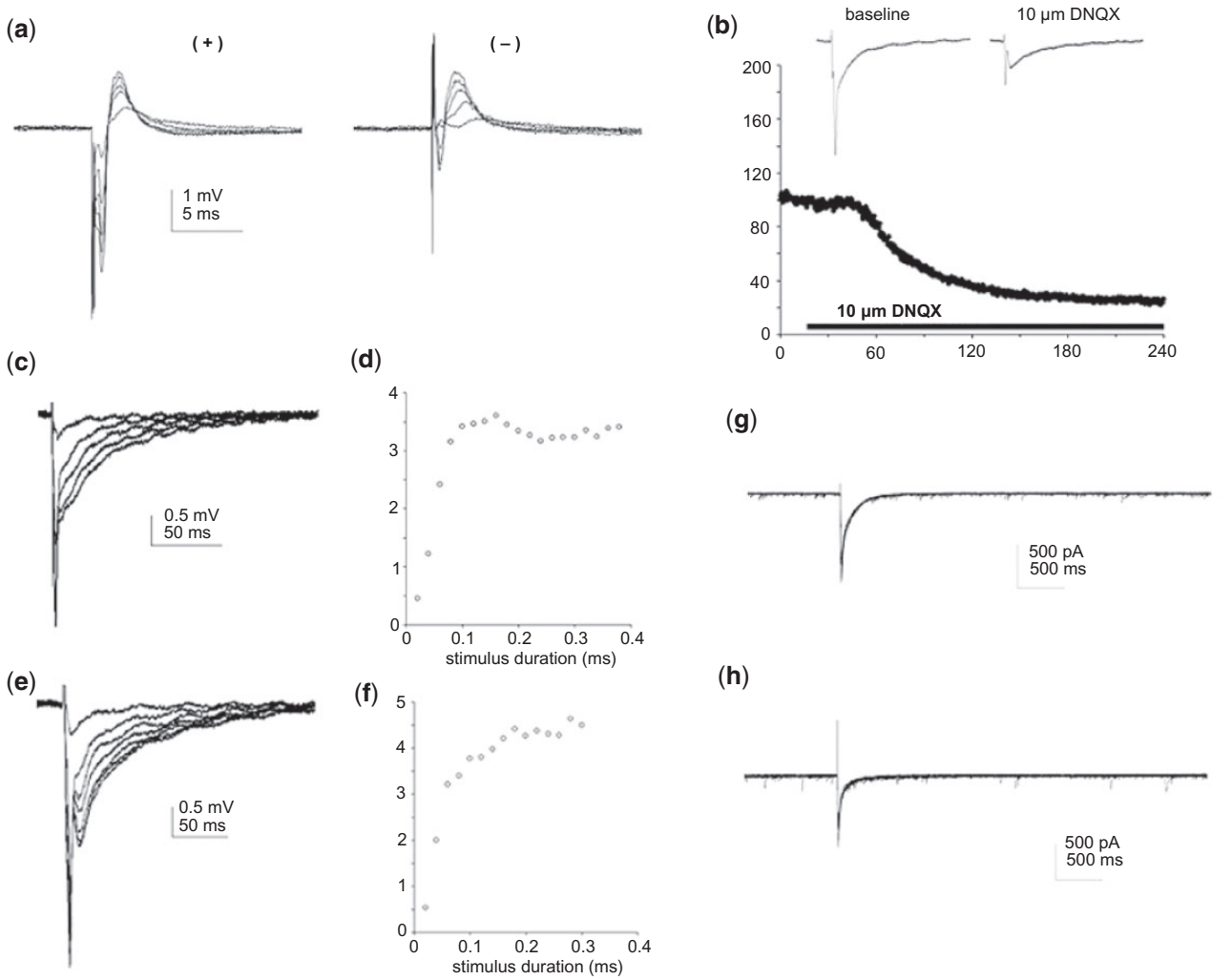

Figure 11. Neuronal electrophysiological responses were not impacted by CX717 treatment. A, Traces of local field responses recorded from the globus pallidus of a CX717-treated rat collected at regular stimulus duration steps (I/O experiment) are overlaid. The positive-going responses were insensitive to stimulus polarity (ie, positive (+) vs negative (–) input current). B, Graph shows fEPSP amplitudes plotted as a function of time. Bath application of the glutamate receptor antagonist DNQX (10 µM) nearly eliminated the fEPSP (traces inset, top), confirming that these are glutamatergic synaptic responses. C, Cortico- striatal synaptic responses of the type described in (B) from a vehicle-treated control animal collected at regular stimulus duration steps are overlaid; D, Graph shows fEPSP amplitude versus stimulation duration steps from I/O experiment in (C). E and F, I/O experiment (same as in panels c and d) for a CX717-treated animal. G and H, Representative IPSC responses, following by spontaneous mini-potentials collected from caudate/putamen neurons by the whole-cell recording technique in slices prepared from vehicle-treated (g) and CX717-treated (H) animals: No differences were detected in response amplitudes.

treatment recovery period for CX717. Importantly, CX717-associated vacuoles were not induced in unfixed frozen sections of brain from CX717-treated rats, indicating that the lesions do not represent evidence of CX717-mediated neurotoxicity. In addition, vacuoles do not occur in brain neuropil of rats treated *in vivo* with other structurally related class II ampakines (CX1739 and CX1763), demonstrating that the change is not a class effect.

Given the fact that vacuoles occur with CX717 only in the presence of formaldehyde and methanol and the literature suggests that N-oxide of CX717 might react with formaldehyde under certain conditions (Acree et al., 1991, Holm, 1987, Seng and Ley, 1972, Woldman et al., 1994), we conducted preliminary experiments to determine the chemical properties of such mixtures. When tested in a cell-free aqueous solution, the experiments revealed that exposure of CX717 to the same formalin/methanol solution used as a fixative in the previous neurohistology analyses produced a substantial heat-producing (7.3°C) reaction. These experiments suggest that CX717-associated vacuoles might result from an exothermic reaction of CX717 reacting with standard histology fixatives containing formaldehyde and methanol, the principal components in commercial formalin and glyoxal preparations. Such a significant exothermic reaction would be capable of vaporizing low-molecular weight components (H_2O, NO, amines, NH_3) to produce gas bubbles within the microenvironment of brain slices, particularly in perivascular regions, producing spatial disruption of the neuropil (ie, vacuolation) via local expansion of the gas. This process may be abetted by astrocyte swelling. This hypothesis merits additional study.

In summary, our robust dataset—including neuropathology assessment, biomarker evaluation, time-course photography, transmission electron microscopy, and chemistry experiments—permit the safety of CX717 and the class II ampakines to be viewed in a new light. Our data indicate that CX717-associated vacuoles do not represent evidence of a genuine

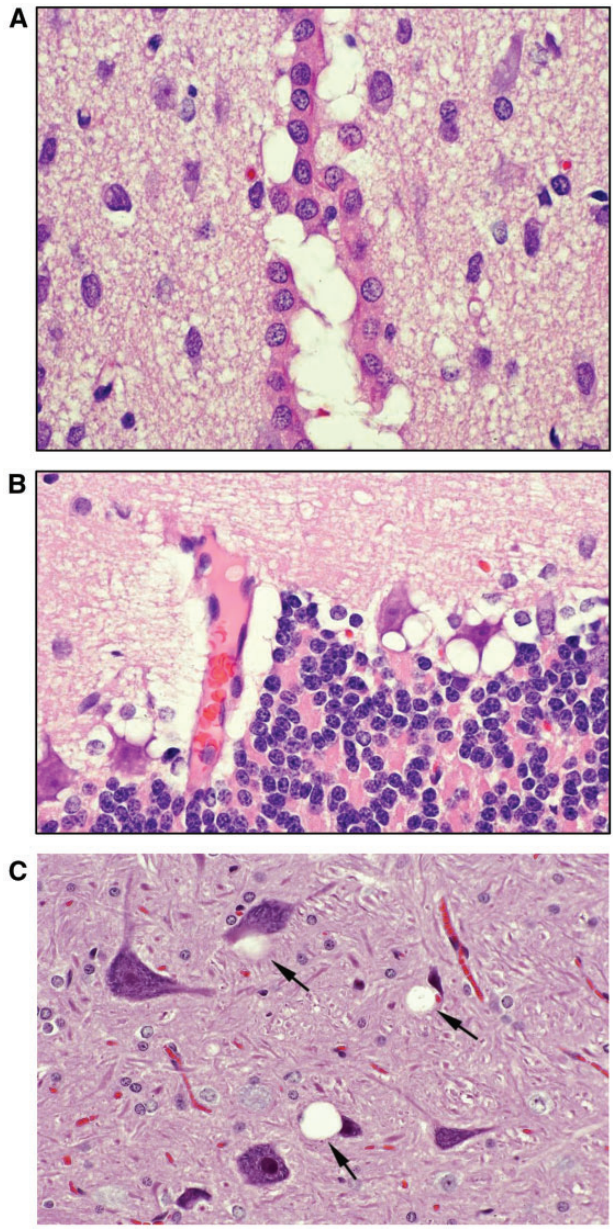

Figure 12. Not all ampakines induce vacuoles. A 4-Week Oral Toxicity Study of CX1739 in Rats with a 4-week Recovery Period. A, High power micrograph of the ependymal lining of the third ventricle in the brain of a control group male rat. The lining is distorted and the ventricle occluded by prominent subependymal vacuoles that represent postmortem alteration and are most likely due to swelling of periventricular astrocytic cell processes. (Rat 1008, Group 1 male; H&E × 410). B, High power micrograph of the cerebellar cortex of a high dose group male rat. Vacuoles are present within the Purkinje cell zone and around blood vessels. These vacuoles undoubtedly represent postmortem swelling of astrocytic processes. Although this micrograph was prepared from the brain of a high dose group rat, similar degrees of vacuolation were present in the cerebella of brains from control group animals. (Rat 1045, Group 4 male; H&E × 410).

neurotoxic effect—and especially an ampakine-induced neurotoxic class effect—but rather are a CX717-specific *postmortem* artifact associated with tissue fixation. Future nonclinical studies may negate the impact of this effect by adjusting the histology processing strategy for brain tissues to avoid routine aldehyde fixation, which drives vacuole formation. Possible adjustments might include rapid brain removal so that some brain regions may be examined as unfixed frozen sections or utilization of fixatives that do include aldehydes for preserving some brain regions. Although such modifications do not yield optimal structural conservation of delicate brain neuropil, they would prevent the generation of CX717-associated vacuoles. The critical take-home message is that the CX717-associated vacuoles do not represent a risk for human patients being treated with agents of this molecular class. Accordingly, the current data should clear the path for continuing clinical research on the use of this promising class of compounds to treat a broad range of currently underserved neurological diseases.

FUNDING

The various studies were funded by research grants issued by RespireRx Pharmaceuticals, Inc.

REFERENCES

Acree, Jr., W. E., Tucker, S. A., Zvaigzne, A. I., Meng-Yan, Y., Pilcher, G., , and Ribeiro Da Silva, M. D. M. C. *J. Chem.* (1991). Enthalpies of combustion of 2, 4, 6-trimethylbenzonitrile, 2, 4, 6-trimethylbenzonitrile *N*-oxide, 2, 6-dimethylbenzonitrile, 2, 4, 6-trimethoxybenzonitrile, and 2, 4, 6-trimethoxybenzonitrile *N*-oxide: the dissociation enthalpies of the (N_O) bonds. *Thermodynamics*, **23**, 31.

Arai, A. C., and Kessler, M. (2007). Pharmacology of ampakine modulators: From AMPA receptors to synapses and behavior. *Curr. Drug Targets* **8**, 583–602.

Arai, A. C., Xia, Y. F., Rogers, G., Lynch, G., and Kessler, M. (2002). Benzamide-type AMPA receptor modulators form two subfamilies with distinct modes of action. *J. Pharmacol. Exp. Ther.* **303**, 1075–1085.

Bolon, B., Garman, R. H., Pardo, I. D., Jensen, K., Sills, R. C., Roulois, A., Radovsky, A., Bradley, A., Andrews-Jones, L., Butt, M., *et al.* (2013). STP position paper: Recommended practices for sampling and processing the nervous system (brain, spinal cord, nerve, and eye) during nonclinical general toxicity studies. *Toxicol. Pathol.* **41**, 1028–1048.

Bélanger, M., and Magistretti, P. J. (2009). The role of astroglia in neuroprotection. *Dialog. Clin. Neurosci.* **11**, 281.

Danysz, W. (2002). CX-516 cortex pharmaceuticals. *Curr. Opin. Investig. Drugs* **3**, 1081–1088.

Fan, D., Grooms, S. Y., Araneda, R. C., Johnson, A. B., Dobrenis, K., Kessler, J. A., and Zukin, R. S. (1999). AMPA receptor protein expression and function in astrocytes cultured from hippocampus. *J. Neurosci. Res.* **15**, 557–571.

Federal Register. (1985). Principles for the Utilization and Care of Vertebrate Animals Used in Testing, Research, and Training. 50(97).

Garman, R. H. (2011). Histology of the central nervous system. *Toxicol. Pathol.* **39**, 22–35.

Garman, R. H., Fix, A. S., Jortner, B. S., Jensen, K. F., Hardisty, J. F., Claudio, L., and Ferenc, S. (2001). Methods to identify and characterize developmental neurotoxicity for human health risk assessment. II: neuropathology. *Environ. Health Perspect.* **109**, 93–100.

Goff, D. C., Lamberti, J. S., Leon, A. C., Green, M. F., Miller, A. L., Patel, J., Manschreck, T., Freudenreich, O., and Johnson, S. A. (2008). A placebo-controlled add-on trial of the Ampakine, CX516, for cognitive deficits in schizophrenia. *Neuropsychopharmacology* **33**, 465–472.

Greer, J., and Ren, J. (2009). Ampakine therapy to counter fentanyl-induced respiratory depression. *Respir. Physiol. Neurobiol.* **168**, 153–157.

Haw, A. J., Meyer, L. C., Greer, J. J., and Fuller, A. (2016). Ampakine CX1942 attenuates opioid-induced respiratory depression and corrects the hypoxaemic effects of etorphine in immobilized goats (Capra hircus). *Vet. Anaesth. Analog.* **43**, 528–538.

Holm, R. H. (1987). Metal-centered oxygen atom transfer reactions. *Chem. Rev.* **87**, 1401.

Ingvar, M., Ambros-Ingerson, J., Davis, M., Granger, R., Kessler, M., Rogers, G. A., Schehr, R. S., and Lynch, G. (1997). Enhancement by an ampakine of memory encoding in humans. *Exp. Neurol.* **146**, 553–559.

Kara, N. Z., Flaisher-Grinberg, S., and Einat, H. (2015). Partial effects of the AMPAkine CX717 in a strain specific battery of tests for manic-like behavior in black Swiss mice. *Pharmacol. Rep.* **67**, 928–933.

Kimelberg, H. K., and Nedergaard, M. (2010). Functions of astrocytes and their potential as therapeutic targets. *Neurotherapeutics* **7**, 338–353.

Kramar, Lin, Lin, Arai, and Lynch, J. (2004). A Novel Mechanism for the Facilitation of Theta-Induced Long-Term Potentiation by Brain-Derived Neurotrophic Factor. *Neurosci* **24**(22), 5151–5161.

Lynch, G., and Gall, C. M. (2013). Mechanism based approaches for rescuing and enhancing cognition. *Front. Neurosci.* **7**, 143.

Oertel, B.G., Felden, L., Tran, P. V., Bradshaw, M. H., Angst, M. S., Schmidt, H., Johnson, S., Greer, J. J., Geisslinger, G., Varney, M. A., and Lötsch. (2010). Selective Antagonism of Opioid-Induced Ventilatory Depression by an Ampakine Molecule in Humans Without Loss of Opioid Analgesia. *J. Clin. Pharmacol. Ther.* **87**(21).

Peters, A., Verderosa, A., and Sethares, C. (2008). The neuroglial population in the primary visual cortex of the aging rhesus monkey. *Glia* **56**, 1151–1161.

Peters, A. (2009). The effects of normal aging on myelinated nerve fibers in monkey central nervous system. *Front. Neuroanat.* **3**, 11.

ICH S6 (R1), (1997). Preclinical safety evaluation of biotechnology-derived pharmaceuticals.

Rastogi, V., Puri, N., Arora, S., Kaur, G., Yadav, L., and Sharma, R. (2013). Artefacts: A diagnostic dilemma – a review. *J. Clin. Diagn. Res.* **7**, 2408–2413.

Ren, J., Poon, B. Y., Tang, Y., Funk, G. D., and Greer, J. J. (2006). Ampakines alleviate respiratory depression in rats. *Am. J. Respir. Crit. Care Med.* **174**, 1384–1391.

Rueda, J. R., Ballesteros, J., and Tejada, M. I. (2009). Systematic review of pharmacological treatments in fragile X syndrome. *BMC Neurol.* **9**, 53.

Seng, F., and Ley, K. A. (1972). Reaction of benzofuroxan with formaldehyde. *Chem. Internat. Edit.* **11**, 1009.

Silverman, J. L., Oliver, C. F., Karras, M. N., Gastrell, P. T., and Crawley, J. N. (2013). AMPAKINE enhancement of social interaction in the BTBR mouse model of autism. *Neuropharmacology* **64**, 268–282.

Strain, S. M., and Tasker, R. A. R. (1991). Hippocampal damage produced by systemic injections of domoic acid in mice. *Neuroscience* **44**, 343–352.

Sun, Y., Olson, R., Horning, M., Armstrong, N., Mayer, M., and Gouaux, E. (2002). Mechanism of glutamate receptor desensitization. *Nature* **417**, 245–253.

Wesensten, N. J., Reichardt, R. M., and Balkin, T. J. (2007). Ampakine (CX717) effects on performance and alertness during simulated night shift work. *Aviat. Space Environ. Med.* **78**, 937–943.

Woldman, Y. Y., Khramtsov, V. V., Grigorev, I. A., Kiriljuk, I. A., and Utepbergenov, D. I. (1994). Spin trapping of nitric oxide by nitronylnitroxides: Measurement of the activity of NO synthase from rat cerebellum. *Biochem. Biophys. Res. Commun.* **202**, 195–203.

Ye, X., and Carp, R. I. (1996). Histopathological changes in the pituitary glands of female hamsters infected with the 139H strain of scrapie. *J. Comp. Pathol.* **114**, 291–304.